Neurochemical Research (2019) 44:1567–1581
https://doi.org/10.1007/s11064-019-02779-4

ORIGINAL PAPER

Mitochondrial Dynamics Impairment in Dexamethasone-Treated Neuronal Cells

Wilasinee Suwanjang[1] · Kay L. H. Wu[2] · Supaluk Prachayasittikul[3] · Banthit Chetsawang[4] · Komgrid Charngkaew[5]

Received: 12 June 2018 / Revised: 14 March 2019 / Accepted: 15 March 2019 / Published online: 19 March 2019

Abstract

Dexamethasone is an approved steroid for clinical use to activate or suppress cytokines, chemokines, inflammatory enzymes and adhesion molecules. It enters the brain, by-passing the blood brain barrier, and acts through genomic mechanisms. High levels of dexamethasone are able to induce neuronal cell loss, reduce neurogenesis and cause neuronal dysfunction. The exact mechanisms of steroid, especially the dexamethasone contribute to neuronal damage remain unclear. Therefore, the present study explored the mitochondrial dynamics underlying dexamethasone-induced toxicity of human neuroblastoma SH-SY5Y cells. Neuronal cells treatment with the dexamethasone resulted in a marked decrease in cell proliferation. Dexamethasone-induced neurotoxicity also caused upregulation of mitochondrial fusion and cleaved caspase-3 proteins expression. Mitochondria fusion was found in large proportions of dexamethasone-treated cells. These results suggest that dexamethasone-induced hyperfused mitochondrial structures are associated with a caspase-dependent death process in dexamethasone-induced neurotoxicity. These findings point to the high dosage of dexamethasone as being neurotoxic through impairment of mitochondrial dynamics.

Keywords Dexamethasone · Mitochondrial dynamics · Mitophagy · Neuron · Cell Death

Introduction

Dexamethasone, a synthetic glucocorticoid receptor agonist, is widely used as a therapeutic and as an agent for testing function of the hypothalamic–pituitary–adrenal (HPA) axis. It has been reported to induce cell death such as striatal cells [1], cerebellar neurons [2] and SH-SY5Y cells [3] and cause apoptosis in the granule cell layer of hippocampus [4], and impairment of cognitive and motor development [5].

The finding of mitochondira dynamics during apoptosis has expanded interest in the molecular mechanisms working behind the structural of these mitochondrial shape changes. It has been demonstrated that mitochondrial functions are regulated by a balance in mitochondrial dynamics between fission and fusion. Dynamin-related protein1 (DRP1), Fission 1 (FIS1), Mitofusin 2 (MFN2) and Optic atrophy 1 (OPA1) are factors that control and maintain mitochondrial dynamics and distribution [6]. The fission of mitochondrial occur in post-mitotic cells, split into small organelles. Excessive mitochondrial fission with exposure of toxin or a lack of fusion, results in the network breakdown mtDNA degradation, respiratory damage, and reactive oxygen species (ROS) over production. Whereas mitochondrial fusion is essential for cellular development and apoptosis protection [7]. However, it has been revealed that inhibition of DRP1 can induce genome dificiency, DNA damage and mitochondrial hyperfusion [8]. It was suggested that the ROS or oxidation might activate mitochondrial fusion [9]. But, this mitochondrial fusion reaction can be inhibited by glutathione (GSH). Failure of mitochondria function has been linked to a variety

✉ Wilasinee Suwanjang
wilasinee.suw@mahidol.ac.th

1 Center for Research and Innovation, Faculty of Medical Technology, Mahidol University, 10700 Bangkok, Thailand

2 Institute for Translational Research in Biomedicine, Kaohsiung Chang Gung Memorial Hospital, Kaohsiung 83301, Taiwan, Republic of China

3 Center of Data Mining and Biomedical Informatics, Faculty of Medical Technology, Mahidol University, 10700 Bangkok, Thailand

4 Research Center for Neuroscience, Institute of Molecular Biosciences, Mahidol University, 73170 Nakhonpathom, Thailand

5 Department of Pathology, Faculty of Medicine, Siriraj Hospital, 10700 Bangkok, Thailand

of diseases such as metabolic [10], Alzheimer's [11], Parkinson's [12], and Huntington's diseases [13] as well as the major depressive disorder [14].

Therefore, healthy mitochondria may be required for neuronal survival, and imbalance in homeostatic processes may lead to neuronal cell death. However, the role of mitochondrial regulation in dexamethasone-induced neurotoxicity is controversial. The current study explored the effects of dexamethasone on mitochondrial dynamics in SH-SY5Y neuroblastoma cell lines. It was proposed that dexamethasone may be a neurotoxic agent, which caused neuronal injury and neurodegenerative disease development.

Materials and Methods

Chemicals and Reagents

SH-SY5Y neuroblastoma cell line was obtained from the American Type Culture Collection (Manassas, VA, USA). Dulbecco's Modified Eagle Medium (DMEM)/ Nutrient Mixture F-12 (Ham) (1:1), fetal bovine serum (FBS), penicillin and streptomycin were purchased from Gibco BRL (Gaithersburg, MD, USA). Cell lysis buffer was obtained from Sigma Aldrich (St. Louis, MO, USA). BCA protein assay kit was supplied with Navogen (Billerica, MA, USA). WST-1 cell proliferation assay kit was obtained from Clontech (Kyoto, Japan). ATP colorimetric assay kit was purchased from BioVision (Milpitas, CA, USA). MitoSOXTM Red superoxide indicator was obtained from Invitrogen. MitoTracker G was purchased from Molecular Probes (Eugene, OR, USA). Primary antibodies used for Western blot including rabbit polyclonal anti-caspase-3, rabbit polyclonal anti-DRP1 (D6C7), rabbit polyclonal anti-pDRP1 (ser616), rabbit polyclonal anti-OPA1 were supplied with Cell Signaling Technology. Rabbit polyclonal anti-FIS1 was purchased from Sigma-Aldrich. Rabbit polyclonal anti-MFN2 (D2D10) and mouse monoclonal anti-GAPDH were purchased from Abcam. Rabbit polyclonal anti-PINK1 was obtained from Cayman Chemical, and rabbit polyclonal anti-Parkin (PRK8) was obtained from Santa Cruz Biotechnology. HRP-conjugated secondary antibody was purchased from Jackson Immuno Research (West Grove, PA, USA). TRIzol reagent was purchased from Invitrogen Life Technologies, (Carlsbad, CA, USA). cDNA using the kit was supplied with Applied Biosystems (Foster City, CA, USA) and antifade reagent in glycerol buffer was purchased from Vector Laboratories (Burlingame, USA).

Culture of SH-SY5Y Neuroblastoma Cell Line

Human neuroblastoma (SH-SY5Y) cells were originally derived from the SK-N-SH cell line. SH-SY5Y cells were maintained in 75 cm^2 flasks with DMEM/F-12, supplemented with 10% heat-inactivated FBS at 37 °C in an atmosphere of 5% CO_2 and 95% air. For the experiments, seeding density of the cells at 2×10^5 cells/mL in 96-well culture plates, 10 cm petri dishes and grown to 70–80% confluence. Before the initiation of treatment, media were replaced with DMEM/F-12 containing 1% (v/v) FBS.

Measurement of Cell Proliferation

The WST-1 assay was used for the measurement of cell proliferation after treatment with dexamethasone. SH-SY5Y cells were plated at 2×10^4 cells/well in 96-well plates and cultured for 24 h prior to use. The control group contained SH-SY5Y cells which were cultured in media without treatment. The dexamethasone was added to the relevant wells in 100 µL volume and incubated with the cells at 37 °C for 6 or 24 h. Then the premixed WST-1 reagent was added to each well and incubated at 37 °C for 1.50 h. The optical density of the solution was measured at 440 nm using a microplate reader.

Measurement of Intracellular ATP Concentration

ATP concentration was determined as described previously [15], using an ATP colorimetric assay kit. Total protein samples from SH-SY5Y cells were centrifuged at 14,000 rpm for 15 min at 4 °C. The supernatants were incubated with ATP reaction mixture for 1 h. The ATP levels were detected at 570 nm using a microplate reader (Thermo Fisher Scientific Inc., Waltham, MA, USA). The assay was linear from 40 to 200 µM for ATP with a coefficient of determination (r^2) > 0.999. Relative ATP content was calculated according to the peak area versus the ATP standard curve. ATP levels were normalized to the protein concentration of samples. Protein concentrations were determined by BCA protein assay kit. All experiments were repeated in duplicate.

Superoxide Detection

The detection of superoxide in live cells was performed using MitoSOX™ Red superoxide indicator. Mitochondria and nuclei were stained with 500 nM MitoTracker Green. Cells were seeded directly on to glass coverslips in 12-well plates at a density of 20,000 cells/well. SH-SY5Y cells were treated with dexamethasone at 1, 2, 5, 10 or 20 µM for 24 h. The control group contained cells and cultured media without treatment. SH-SY5Y cells were incubated with 3.75 µM MitoSOX™ for 30 min prior to the end of the experimental period. After these 30 min, cells were washed three times in 0.1 M PBS. The coverslips were then fixed in 4% paraformaldehyde, mounted with a coverslip and visualized under Fluorescence FV10i microscopy (Olympus, Tokyo, Japan).

The superoxide production was measured using the fluorescence intensity relative to the cell area through Image J software.

Western Immunoblotting

SH-SY5Y cells were lysed by the addition of cell lysis buffer with protease inhibitor cocktail, and scraped off the petri dishes. The samples were sonicated for 10 s and centrifuged at 14,000 rpm for 15 min at 4 °C. Supernatants were collected at -80 °C and proteins were determinated by BCA protein assay kit. Ten milligrams protein samples were subjected to sodium dodecyl sulfate–polyacrylamide gel electrophoresis (SDS-PAGE): 12% gel for caspase-3, FIS1, PINK1 and OPA1; 8% gel for Parkin, pDRP1, DRP1 and MFN2. GAPDH is considered a constitutive housekeeping protein and was used to normalize changes in specific protein expression. The separated protein were transferred to polyvinylidene difluoride (PVDF) membranes. These membranes were incubated with the primary antibodies at 4 °C overnight, and then incubated with HRP-conjugated secondary antibody for 1.50 h. The blots were developed with Chemiluminescent ECL Plus Western Blotting detection reagents and exposed to X-ray films (Fiji, Japan).

RNA Purification and Real-Time Quantitative RT-PCR

Total RNA was extracted from the samples SH-SY5Y cells using TRIzol reagent according to the manufacturer's protocol, and then RNAs were reverse transcribed to cDNA using the kit. The specific primers and TaqMan probes used to analyze the mRNA expression of the mitochondrial dynamic genes related to fission and fusion were ordered from Purigo Biotech, Taiwan. OPA1, DRP1, PINK1 and Parkin were examined in SH-SY5Y cells. The primers for the PCR reaction are listed in Table 1. Human GAPDH, an endogenous control gene, was used as the reference gene. Briefly, PCR reactions were set up in 96-well reaction plates and were run on an ABI 7500 real-time PCR system (Applied Biosystems). The relative of gene expression was normalized against respective controls. The gene expression data were calculated by using $2^{\Delta\Delta Ct1}$ method.

Immunocytochemistry

SH-SY5Y cells were cultured in 24 well plate on sterile glass coverslips at 37 °C for 24 h and then exposed to dexamethasone for 24 h. Whereas the control cells were incubated with culture medium for 24 h. Following this, the cells were incubated with MitoTracker®Green at 500 nM for 30 min. Cells were fixed with 4% paraformaldehyde for 15 min at 4 °C and permeabilized with PBST for 10 min at room temperature and rinsed with PBS three times. Non-specific, antibody binding sites on the cells were blocked by incubating with 5% donkey serum in PBST for 2 h at room temperature. The cells were subsequently incubated with primary antibody against MFN2 (1:250 in PBS) or OPA1 (1:250 in PBS) at 4 °C overnight, followed by incubation in Alexa 594 with donkey anti-rabbit IgG (1:750 in PBST) for 2 h at room temperature. After three washing steps with PBS, followed by incubating with DAPI (1:1000 in PBST) for 20 min. Stained slides were mounted using antifade reagent in glycerol buffer and observed with Fluorescence FV10i microscope (Olympus, Tokyo, Japan).

Table 1 Specific primers for PCR reaction

Primers		Sequences
DRP1	Forward primer	5′-TGCTTCCCAGAGGTACTGGA-3′
	Reverseprimer	5′-TCTGCTTCCACCCCATTTTCT-3′
OPA1	Forward primer	5′-TGTGCCTGACATTGTGTGGG-3′
	Reverse primer	5′- GTCTTCTGAACTAGGAAG GGCT-3′
GAPDH	Forward primer	5′-GAAAGCCTGCCGGTGACTAA-3′
	Reverse primer	5′-AGGAAAAGCATCACCCGGAG-3′
PINK1	Forward primer	5′-TTGCCCCTAACACGAGGAAC-3′
	Reverse primer	5′-ACGTGCTGACCCATGTTGAT-3′
Parkin	Forward primer	5′-TCTCTTGGTTTCACGGTTGGT-3′
	Reverse primer	5′-CTGCACAGCCAGTGAACAAT-3′

Transmission Electron Microscopy (TEM) Assay

Following the experimental treatment, cells were fixed with 4% phosphate-buffered glutaraldehyde following a standard protocol for fixation, dehydration and embedding described previously [16]. Finally, ultrathin transverse sections (95–100 nm) were post-stained with uranyl acetate. The ultrastructure of neuronal cell was observed under a transmission electron microscope (JEOL, Tokyo, Japan).

Mitochondrial Movement

To label mitochondria, SH-SY5Y cells were incubated with 500 nM MitoTracker®Green in medium at 37 °C for 1 h under 5% CO_2 atmosphere. Mitochondrial dynamics were imaged with a time-lapse microscope incubator (Cell^R, Olympus) at 37 °C (5% CO_2). The mitochondria were visualized through an oil immersion (60x) objective lens.

Statistical Analysis

Data were expressed as the mean ± S.E.M. Significance was assessed by independent *t*-test, 2-way analysis of variance (ANOVA) and then Tukey's for specific pairwise comparisons when significant interactions are observed using

the scientific software GraphPad Prism. A value of probability (P) less than 0.05 was considered to be statistically significant.

Results

Effect of Dexamethasone on Cell Viability of SH-SY5Y Cells

To investigate the optimal concentration and incubation period of dexamethasone-induced toxicity. Cell proliferation was assessed after dexamethasone treatment using the WST-1 assay. Treatment of dexamethasone at 2, 5, 10 and 20 μM for 6 h significantly decreased cell proliferation to 78.34 ± 3.90% ($P < 0.05$), 75.23 ± 2.79% ($P < 0.01$), 71.02 ± 4.85% ($P < 0.01$) and 65.07 ± 5.57% ($P < 0.001$), respectively, compared with untreated controls. Treatment with 1, 2, 5, 10 and 20 μM dexamthasone for 24 h significantly decreased cell proliferation to 79.53 ± 2.66% ($P < 0.01$), 71.70 ± 3.82% ($P < 0.001$), 68.20 ± 2.66% ($P < 0.001$), 67.39 ± 2.71% ($P < 0.001$) and 60.95 ± 4.41% ($P < 0.001$), respectively. These results indicate that treatment of the cells with dexamethasone decreased cell proliferation in SH-SY5Y cells with dose-and time-dependent manners (Fig. 1).

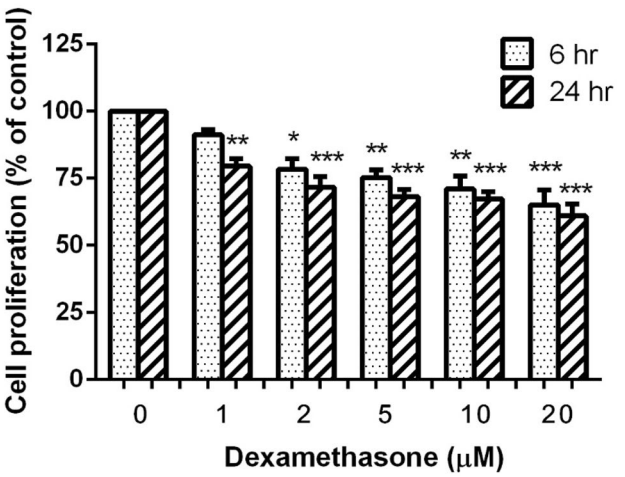

Fig. 1 Effect of dexamethasone-induced reduction in cell proliferation. SH-SY5Y cells were treated with various concentrations of dexamethasone for 6 and 24 h. The control-cultured cells (0 μM dexamethasone) were incubated with culture medium for 6 and 24 h. Cell proliferation was measured using WST-1 assay. The results are expressed as mean ± S.E.M. of four independent experiments. Two-way analysis of variance (ANOVA) and then Tukey's for specific pairwise comparisons were performed for statistical analysis. *$P < 0.05$, **$P < 0.01$ and ***$P < 0.001$ compared with the control

Effect of Caspase-3 Activation on Dexamethasone-Treated SH-SY5Y Cells

Caspase-3 is the cysteine proteases with activities implicated in apoptosis. Activation of pro-caspase-3 (35 kDa) provides cleaved active forms, subunits of 19 and 17 kDa. Treatment of SH-SY5Y cells with dexamethasone at 10 or 20 μM for 6 or 24 h significantly increased caspase-3 (19 kDa) to 114.10 ± 0.88% (20 μM for 6 h; $P < 0.01$), 123.5 ± 8.69% (20 μM for 24 h; $P < 0.01$), and significantly increased the 17 kDa form of caspase-3 to 116.50 ± 5.12% (20 μM for 6 h; $P < 0.01$) and 120.30 ± 3.68% (10 μM for 24 h; $P < 0.05$), 129.10 ± 5.83% (20 μM for 24 h; $P < 0.01$). Therefore, the results showed that dexamethasone upregulated caspase-3 expression in a dose-dependent manner (Fig. 2).

Dexamethasone-Induced Decrease of Intracellular ATP Concentration

Effect of dexamethasone on intracellular ATP content was detected by ATP colorimetric assay kit. Cells treated with 1, 2, 5, 10 and 20 μM of dexamethasone for 6 h decreased the intracellular ATP to 38.07 ± 1.24 nM/μg (1 μM), 32.65 ± 1.07 nM/μg (2 μM), 27.61 ± 4.61 nM/μg (5 μM; $P < 0.05$), 31.73 ± 6.58 nM/μg (10 μM) and 30.56 ± 2.13 nM/μg (20 μM) of the basal levels (0 μM; 60.96 ± 10.64 nM/μg), respectively. Whereas SH-SY5Y cells treated with 1, 2, 5, 10 and 20 μM for 24 h decreased the intracellular ATP to 28.90 ± 0.89 nM/μg (1 μM; $P < 0.01$), 30.86 ± 2.38 (2 μM; $P < 0.01$), 36.48 ± 0.15 (5 μM; $P < 0.05$), 39.84 ± 3.78 (10 μM) and 33.08 ± 3.61 nM/μg (20 μM; $P < 0.05$) of the basal levels (0 μM; 57.83 ± 8.48 nM/μg), respectively. Decreases in the intracellular ATP in the presence of dexamethasone were statistically significant at 5 μM for 6 h, and at 1, 2, 5 and 20 μM for 24 h (Fig. 3).

Dexamethasone-Induced Mitochondrial ROS Generation

This study investigated the effect of dexamethasone on ROS production in mitochondria. The cells were treated with different concentrations (0–20 μM) of dexamethasone for 24 h. The SH-SY5Y cells were incubated with MitoTracker Green for 1 h and stained with MitoSOX™ Red for 30 min. The MitoSOX-red was used to assay the presence of superoxide specifically generated from the mitochondria. Results revealed that the intensity of MitoSOX-red in dexamethasone-treated cells was increased compared to the dexamethasone-untreated (native) control cells (Fig. 4).

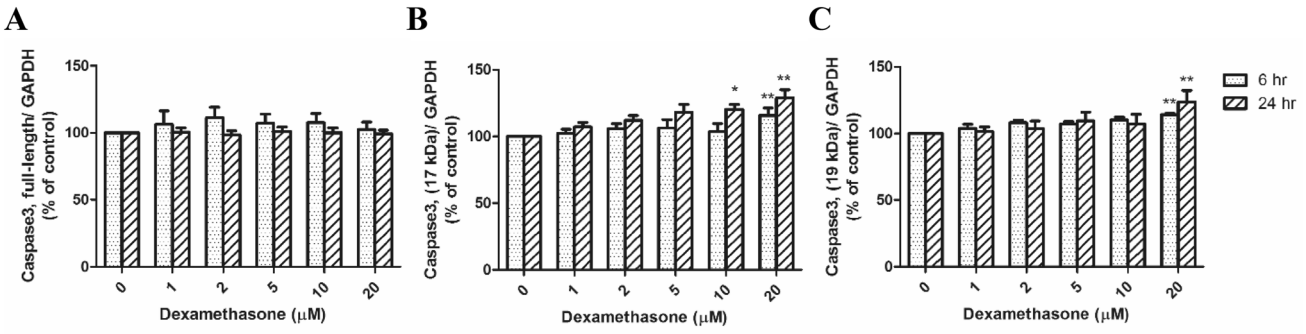

Fig. 2 Effect of dexamethasone treatments on caspase-3 and cleaved caspase-3 levels. SH-SY5Y cells were treated with 1, 2, 5, 10 and 20 μM dexamethasone for 6 and 24 h. The levels of caspase-3 and cleaved caspase-3 were determined using Western blot analysis. Protein bands for each regimen were quantified by densitometry, and their differences are represented in graph as a ratio of caspase-3 (35 kDa) and cleaved caspase-3 (19 and 17 kDa) over GAPDH bands. Values represent mean ± S.E.M. of four independent experiments. Two-way analysis of variance (ANOVA) and then Tukey's for specific pairwise comparisons were performed for statistical analysis. $^{*}P < 0.05$ and $^{**}P < 0.01$ compared with the control-untreated cells

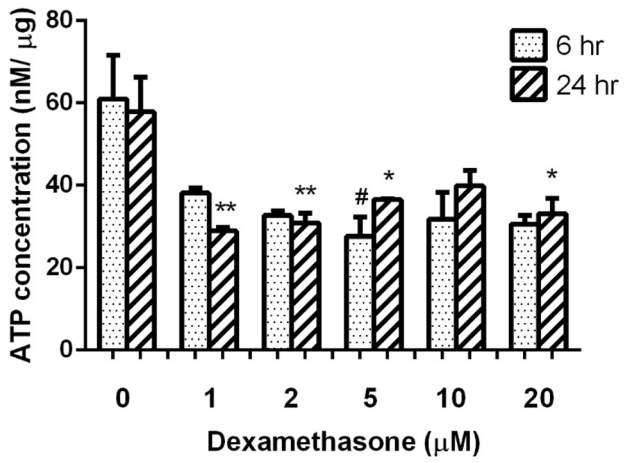

Fig. 3 Effect of dexamethasone on intracellular ATP content in SH-SY5Y cells. Cells were treated with various concentrations of dexamethasone for 6 and 24 h. Intracellular ATP content was determined using ATP colorimetric assay kit. Values represent mean ± S.E.M. of three independent experiments. Two-way analysis of variance (ANOVA) and then Tukey's for specific pairwise comparisons were performed for statistical analysis. $^{*}P < 0.05$ and $^{**}P < 0.01$ compared with the control (0 μM)

Dexamethasone-Altered Mitochondrial Dynamics: Protein Levels

The morphological dynamics of mitochondria that can divide (fission) and fuse (fusion) to form globular or tubular networks within cells. Homeostasis in healthy mitochondria is regulated by the relative roles of fission and fusion proteins. Dexamethasone-induced alterations in fission proteins (DRP1, pDRP1 and FIS1) and fusion proteins (OPA1 and MFN2) were determined in the neuroblastoma SH-SY5Y cells using Western blot analysis.

The results showed that dexamethasone at 2, 5, 10 and 20 μM for 6 h significantly reduced the amount of pDRP1 expression to 77.91 ± 5.46% ($P < 0.05$), 79.84 ± 2.78% ($P < 0.05$), 84.69 ± 2.99% ($P < 0.05$), and 49.49 ± 6.25% ($P < 0.001$), respectively, compared with the control value. In addition, dexamethasone at 10 and 20 μM for 24 h significantly decreased the amount of pDRP1 expression to 85.30 ± 3.79% ($P < 0.01$) and 82.27 ± 3.42% ($P < 0.01$), respectively, compared with the control value (Fig. 5a). Fission protein DRP1 significantly decreased to 84.14 ± 2.61% ($P < 0.05$) at 24 h in 20 μM dexamethasone-treated cells (Fig. 5b). Another mitochondrial fission protein, FIS1, also was determined. It was found that dexamethasone at 10 and 20 μM for 24 h significantly decreased the FIS1 protein levels to 80.86 ± 5.78% ($P < 0.01$) and 79.74 ± 3.45% ($P < 0.01$), respectively, compared with the control values (Fig. 5c). This agrees with our previous study that dexamethasone treatment significantly increases fusion protein expression [16]. However, the reduction of FIS1 expression results in mitochondrial dynamic changes, including a reduction of fission and in mitochondrial elongation [19]. These data indicate that mitochondrial fission is suppressed in response to dexathansone, and that the association of DRP1 with mitochondria might be regulated by the ATP content of neuronal cells.

Dexamethasone-induced alterations of mitochondrial fusion protein expression was tested in SH-SY5Y cells. The large GTPases, OPA1 and MFN2 play a role in the fusion aspect of mitochondrial dynamic processes. OPA1 is localized on the inner mitochondrial membrane and associated with the inner mitochondrial membrane fusion. The various form of OPA1 are different in long and short forms. The short forms of OPA1 are more loosely attached to the inner mitochondrial membrane which retain a hydrophobic domain. Therefore two bands of OPA1, 92 and 111 kDa,

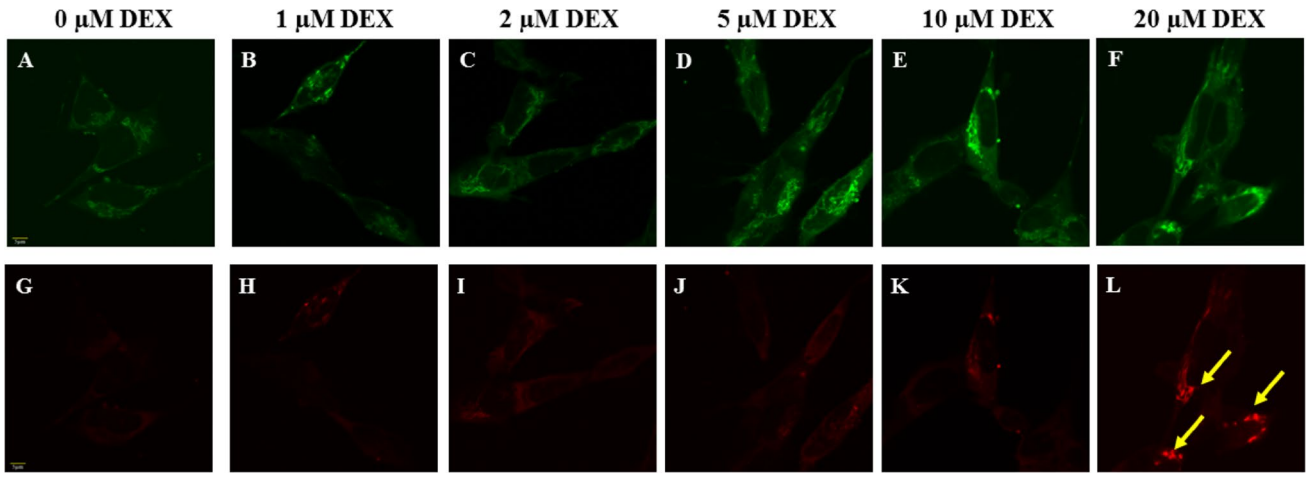

Fig. 4 Effect of dexamethasone on the formation of ROS. SH-SY5Y cells were treated with 20 μM dexamethasone (DEX) for 24 h. ROS production was detected by the intensity of MitoSOX^{TM}Red fluorescence. The mitochondria was stained with MitoTracker Green and observed under confocal microscope

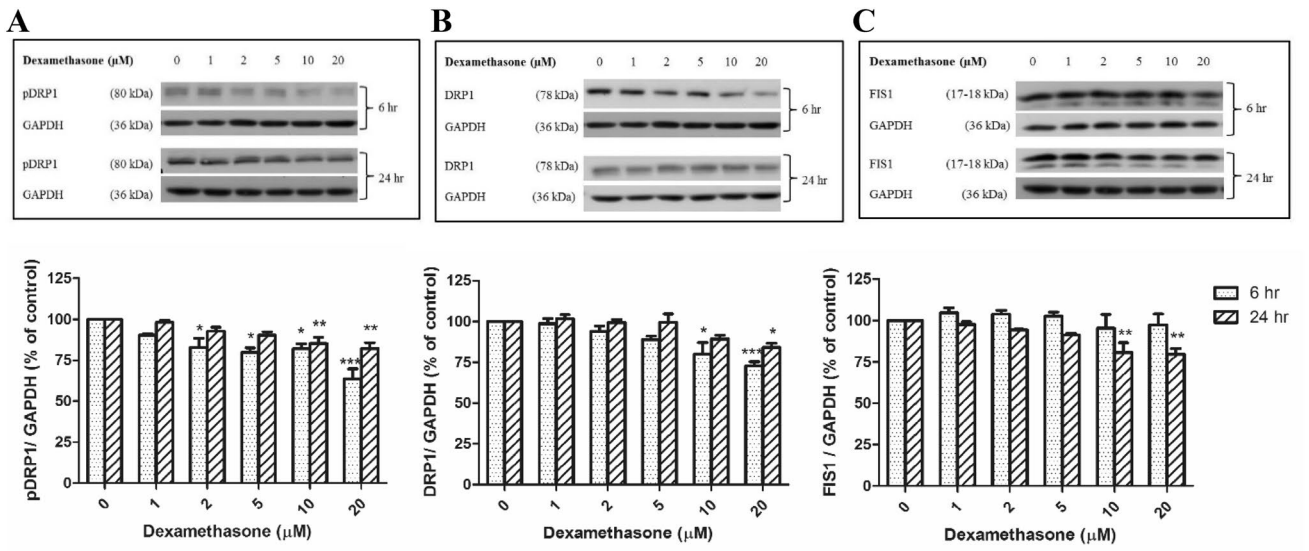

Fig. 5 Effect of dexamethasone-induced alterations in levels of pDRP1, DRP1 and FIS1 proteins in SH-SY5Y cells. Cells were treated with various concentrations of dexamethasone for 6 and 24 h. The levels of pDRP1, DRP1 and FIS1 were determined using Western blot analysis. Protein bands for each regimen were quantified by densitometry, and their differences are represented in graph as a ratio of pDRP1, DRP1 or FIS1 over GAPDH bands. Values represent mean ± S.E.M. of four independent experiments. Two-way analysis of variance (ANOVA) and then Tukey's for specific pairwise comparisons were performed for statistical analysis. $^{*}P<0.05$, $^{**}P<0.01$, $^{***}P<0.001$ compared with the control-untreated cells

were examined. Another fusion protein, mitofusion (MFN1 and MFN2) are resided in the outer mitochondrial membrane (OMM). MFN2 triggers aggregation of mitochondria into tight networks through close interaction between OMMs, followed by outer membrane fusion that results in the mitochondrial formation. Exposure with 5, 10 and 20 μM dexamethasone for 24 h significantly increased the expression of OPA1 (92 kDa) to 110.65 ± 3.35% ($P<0.05$), 117.14 ± 1.18% ($P<0.001$) and 126.49 ± 1.83% ($P<0.001$), respectively, compared with the control values (Fig. 6a). Dexamethasone at 10 and 20 μM for 24 h significantly elevated the amount of MFN2 to 129.30 ± 4.36% ($P<0.01$) and 143.86 ± 7.81% ($P<0.001$), respectively, compared with control values (Fig. 6c). However, dexamethasone treatment for 6 h did not show any significant changes in concentration of mitochondrial fusion proteins (neither OPA1 nor

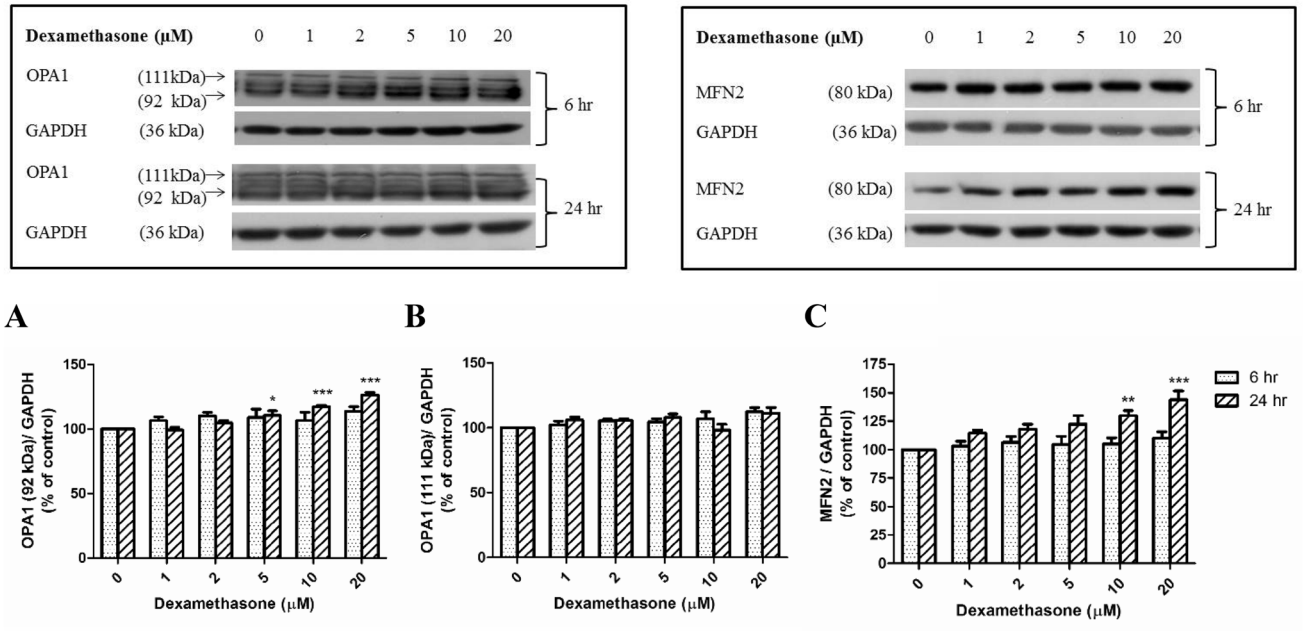

Fig. 6 Effect of dexamethasone-induced alterations in OPA1 and MFN2 proteins levels in SH-SY5Y cells. Cells were treated with various concentrations of dexamethasone for 6 and 24 h. The levels of OPA1 and MFN2 were determined using Western blot analysis. Protein bands for each regimen were quantified by densitometry and their differences are represented in graph as a ratio of OPA1 or MFN2 over GAPDH bands. Values represent mean ± S.E.M. of four independent experiments. Two-way analysis of variance (ANOVA) and then Tukey's for specific pairwise comparisons were performed for statistical analysis. $^{*}P < 0.05$, $^{**}P < 0.01$, $^{***}P < 0.001$ compared with the control untreated cells

MFN2). The results suggested that dexamethasone exposure for 24 h induced mitochondrial fusion by the induction of OPA1 (92 kDa) and MFN2 protein levels. In this regard, the alteration of MFN2 and OPA1 expressions mediated the ubiquitin proteosome pathway in dexamethasone-treated SH-SY5Y cells. However, mitochondrial fusion induced by OPA1 (111 kDa) was not observed (Fig. 6b).

Mitochondrial fluorescent staining dye and immunofluorescence staining were used to mark the induction of mitochondrial fusion in dexamethasone-treated SH-SY5Y cells. Molecular Probe (MitoTracker®), a green-fluorescence dye, was used for staining mitochondria in live SH-SY5Y cells; Mitochondria accumulation was dependent upon mitochondrial membrane potential. Whereas, the immunofluorescence staining was used to demonstrate mitochondrial fusion proteins (OPA1 and MFN2). The colors indicate the active mitochondrial site (green) and mitochondrial fusions (OPA1 and MFN2, red) immunostaining in SH-SY5Y cells. The results of immunofluorescence staining showed increased OPA1 and MFN2 after treatment with dexamethasone compared with the untreated control cells. In co-localization studies, mitotracker green-labeled mitochondria were presented in MFN2- and OPA1-labeled mitochondrial fusion in SH-SY5Y cultured cells (Fig. 7). Therefore, the ultrastructure of mitochondria was compared with the control and dexamethasone-treated cells. After exposure of dexamethasone to the cells, the images showed significant changes in morphological characteristices. The mitochondria appeared as tubular in shape, with a loss of internal membrane structure (Fig. 8c, d). In contrast, the mitochondria of control SH-SY5Y cells were round and regular in shape (Fig. 8a, b).

Dexamethasone-Altered Mitochondrial Dynamics: mRNA Levels

To explore the correlation between mitochondrial dynamic protein levels and mRNA levels, the incubation of SH-SY5Y cells with 20 μM dexamethasone for 24 h was measured using quantitative real-time PCR. The relative OPA1 mRNA levels increased significantly to 1.42 ± 0.11 ($P < 0.05$) compared with levels in untreated-cells (0.91 ± 0.08) (Fig. 9a). Additionally, mitochondrial mRNA levels of fission protein DRP1 did not change significantly in dexamethasone-treated cells (Fig. 9b).

PINK1 and PARKIN in SH-SY5Y Cells Treated with High-Dose Dexamethasone

The previous section imply that dexamethasone at high concentrations can cause alteration of mitochondria dynamics and reduction in ATP content of SH-SY5Y cells. The quality control of mitochondrial is achieved through the fission

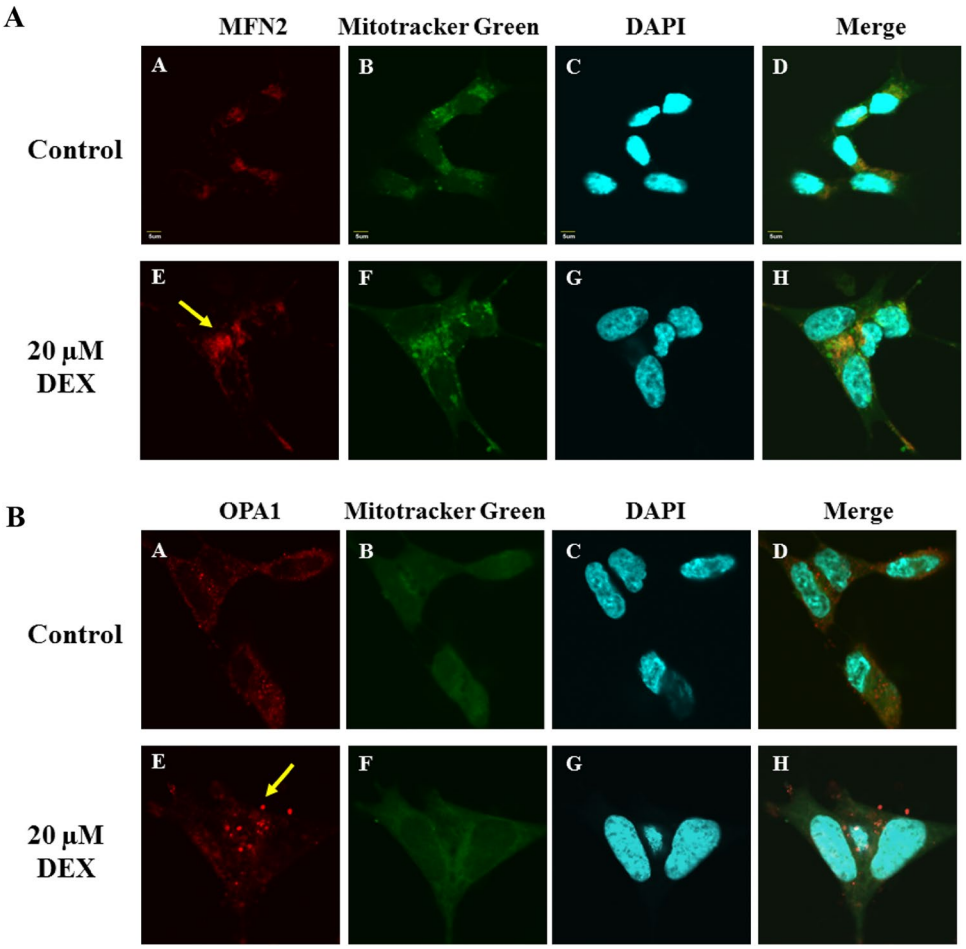

Fig. 7 Fluorescence microscopic images of SH-SY5Y cells demonstrating the effect of dexamethasone (DEX) treatment on fusion mitochondria (MFN2 (**a**) and OPA1 (**b**)) in SH-SY5Y cultured cells. The control-cultured cells were incubated with culture medium for 24 h (**a**–**d**). Some of the control-cultured cells were treated with 20 μM DEX for 24 h (E-H). Cells were incubated with MitoTracker®Green, and then were fixed with 4% paraformaldehyde and stained with rabbit polyclonal antibody against MFN2 or OPA1. The red color indicates MFN2 or OPA1 immunostatining using alexa 549 conjugated donkey anti-rabbit IgG (**a, e**), the red color indicates mitochondrial sites using MitoTracker®Green (**b, f**) and the blue color indicates nucleus sites using DAPI staining. The triple fluorescence (merge) images are shown in D and H. Scale bar = 5 μM

and fusion processes. The fragmented mitochondria can fuse with healthy mitochondria to repair the necessary components for maintaining mitochondrial function through a mitophagy process. Components of mitochondrial quality control include PINK1 and PARKIN expressions.

To assess the correlation of PINK1 and PARKIN expressions with ATP content in high-dose dexamethasone-treated SH-SY5Y cells. The SH-SY5Y cells were incubated with different concentrations of dexamethasone for 6 or 24 h. It was observed that treatments with 5, 10 and 20 μM dexamethasone for 24 h caused significant decreases in the expression of PINK1 protein to 86.77 ± 2.20% ($P < 0.001$), 79.76 ± 1.63% ($P < 0.001$), and 74.57 ± 1.60% ($P < 0.001$), respectively, compared with the control cells (100%) (Fig. 10a, c). Treatment with 20 μM dexamethasone for 6 and 24 h, significantly increased the expression of PARKIN protein to 117.30 ± 3.75% ($P < 0.05$) and 128.20 ± 10.23% ($P < 0.05$), respectively, compared with control values (Fig. 10b, d). The results indicated that the amount of PARKIN levels exhibit their responses to the level of ATP content under high-dose dexamethasone treatment in SH-SY5Y cells. Both PINK1 and PARKIN mRNA levels at 24 h were significantly up-regulated to 1.33 ± 0.08 ($P < 0.01$) and to 1.72 ± 0.07 ($P < 0.05$) compared with the control 0.91 ± 0.06 and 1.01 ± 0.07, respectively (Fig. 10e, f).

Mitochondrial Dynamic Defects in Dexamethasone-Treated SH-SY5Y Cells

To determine whether dexamethasone altered mitochondrial movement, confocal cell^R time-lapse imaging of 20 μM dexamethasone-treated SH-SY5Y cells with mitotracker staining was employed. The mitochondria stained as green is shown in Fig. 11. Mitochondria in the control cells exhibited a spherical structure and distributed within the cytoplasm and cellular processes. At 6 and 24 h after dexamethasone exposures, organelles of SH-SY5Y cells appeared as elongated tubular structures. These data raised the possibility that dexamethasone disrupted mitochondrial quality control and caused the accumulation of mitochondrial fusion proteins in neuronal SH-SY5Y cells (Fig. 11).

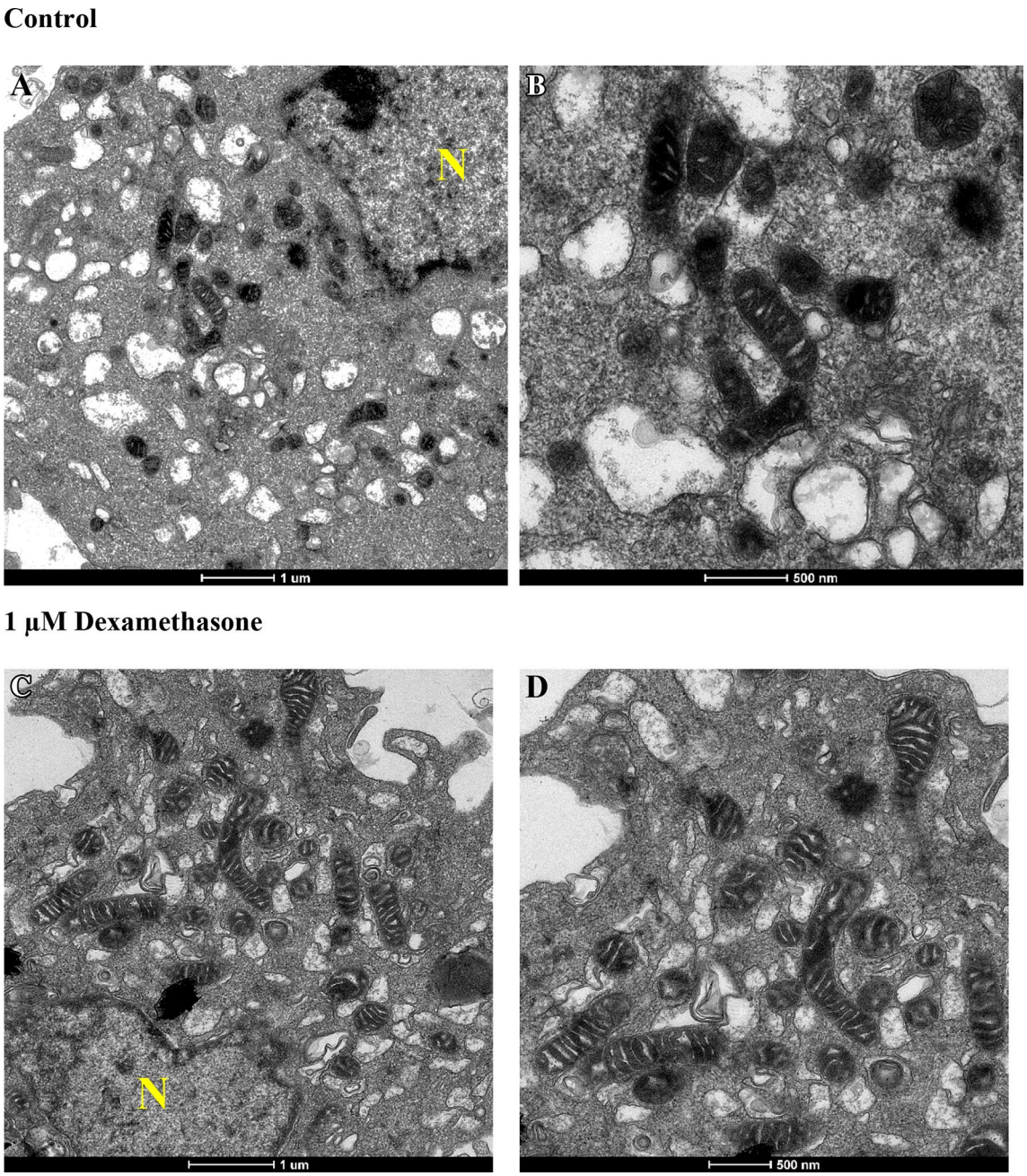

Fig. 8 Morphological changes of SH-SY5Y cells. **a, b** Cells in the control group retained a normal ultrastructure, **c, d** Cell in dexamethasone treatment contained tubular and hazy mitochondrial structure

Discussion

Dexamethasone has proven efficacy for the treatment of many diseases such as spinal cord injury [17], inflammation [18, 19], renal disease [20], seizures [21] and retinal disease [22]. The minimum concentration of dexamethasone was chosen, because previous studies reported that dexamethasone induced neuronal cell death at 1 µM [23–25]. In addition, dexamethasone is reported to damage tendon structures [26] and articular chondrocytes [27], and to cause osteoporosis [28]. In this study, several parameters such as cell proliferation, ATP production, oxidative stress and mitochondrial dynamic markers were studied to confirm the neurotoxicity of dexamethasone on cultured neuronal cells. Incubation of the cells for 24 h with dexamethasone resulted in progressively reduced cell proliferation. Recent studies show that dexamethasone treatment in vivo decreases cell proliferation, and increases cell death [29–33]. These effects

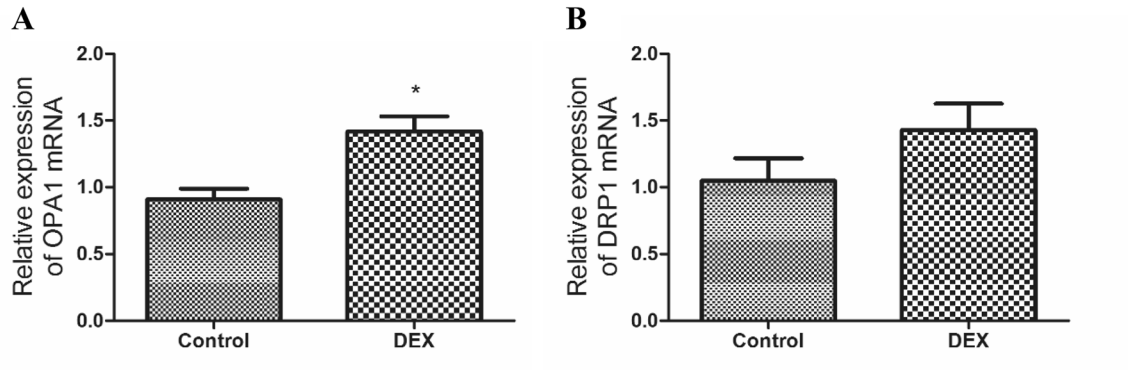

Fig. 9 Relative mitochondrial dynamic, fusion (OPA1, **a**) and fission (DRP1, **b**) mRNA expressions in SH-SY5Y cells. OPA1 and DRP1 mRNA levels were measured by quantitative real-time PCR. Relative expression was determined against GAPDH mRNA levels, and data are expressed as mean ± S.E.M. of four independent experiments. Independent t-test was performed for statistical analysis. $*P < 0.05$ compared with the control-untreated cells

can result in brain damage, behavioral changes and cognitive disabilities.

In this study, the concentration of dexamethasone that reduced cell proliferation also can cause neuronal cell death as indicated by the alteration of biochemical parameters. Caspase-3, found in the mitochondria, cytosol and nucleus, plays a critical role in the degradation of crucial regulatory structures and the intracellular suicide cascade [34–36]. However, the mechanism of dexamethasone-induced neuronal cell death is not clearly understood. It has been suggested that dexamethasone exposure leads to an excessive calcium level which induces caspase cascade activation and cell death [16, 23, 37]. Dexamethasone is reported to cause DNA damage via oxidative stress [38]. It was documented that dexamethasone is able to induce the expression of leucine-rich repeat kinase2 (LRRK2) and α-synuclein which are associated with Parkinson's disease [39]. Alternatively, dexamethasone-induced apoptosis may occur through upregulation of pro-death proteins and/or down-regulation of pro-survival proteins [40, 41].

A number of studies have shown the change of ATP concentration in neurons [42–44]. It has been reported that ATP depletion may be associated with the early effect of the oxidative stress. During the early stages of neuronal cell damage, the calcium accumulation and ATP production are related to the ROS concentration [45, 46]. Decreased ATP concentration has been linked to neurodegenerative diseases such as Alzheimer's [47–49] and Parkinson's diseases [50, 51]. In addition, the elevated level of ROS can be resulted from metabolic activity, mitochondrial dysfunction or peroxisome activity, and lead to the pathological oxidative damage [52].

Mitochondria serve as the main producer of ATP as well as the center for biosynthetic processes in most eukaryotic cells. The networks among mitochondria are important for maintaining integrity and material of mitochondrial DNA. Mitochondrial dynamics refer to the changes in mitochondrial shape, which occur through fission and fusion. These dynamics play important roles in the development and regulation of neuronal functions as well as in the homeostasis of bioenergetics metabolism. Recent findings suggest that excessive mitochondrial fission and fusion occur in large-scale of human diseases, and involve in ultrastructural changes, increased ROS production, declined ATP level, activation of several pro-apoptotic factors, mtDNA deletions, impaired Ca^{2+} buffering, and loss of mitochondrial membrane potential [53–60].

In the present study, dexamethasone exposure can lead to mitochondrial dysfunction as indicated by the decrease in the mitochondrial fission proteins, DRP1 and FIS1. Phosphorylation of DRP1 at serine 616 is the common DRP1 post-translational modification and is mediated by multiple kinases [61–63]. These results confirmed that dexamethasone decreased DRP1 translocation which is regulated by Ser616 phosphorylation. A number of studies have shown that mitochondrial fission is an early event during the process of neuronal cell death [64, 65]. Consistent with our previous study, dexamethasone reduced DRP1 and FIS1 in neuroblastoma SH-SY5Y cells as indicated by the Western blotting [16]. However, inhibition of mitochondrial fission protein does not prevent the activity of BAX/BAK-dependent apoptosis [66]. The possibility that the loss of mitochondrial fission impaired the generation of energy needed for metabolism and induced neuronal degeneration [67]. Some existing evidence show that DRP1 is recruited to mitochondria for membrane construction by interaction with FIS1 [68]. Mitochondrial fusion is governed by MFN 1 and 2 at the outer mitochondrial membrane, and by OPA1 at the inner mitochondrial membrane. Recent studies indicate that MFN2 stimulates cell respiration, substrate oxidation and oxidative phosphorylation subunit expression [69, 70]. Thus, abnormal mitochondrial fusion is reported to

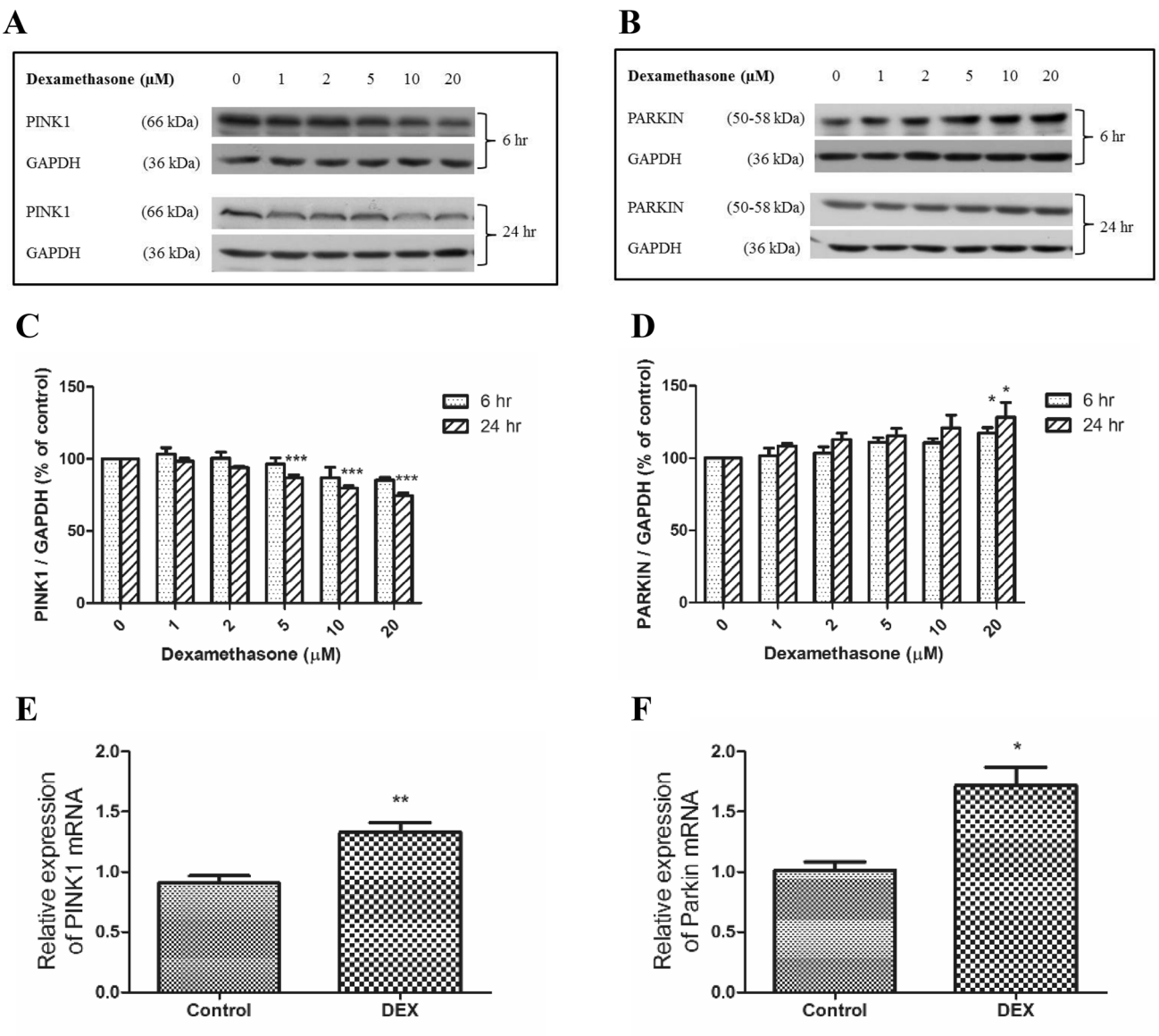

Fig. 10 Effect of dexamethasone-induced alterations of PINK1 and PARKIN levels in SH-SY5Y cells. Cells were treated with various concentrations of dexamethasone for 6 and 24 h. The levels of PINK1 and PARKIN were determined using Western blot analysis. Protein bands for each regimen were quantified by densitometry, and their differences are represented in graph as a ratio of PINK1 or PARKIN over GAPDH bands. The mRNA levels were measured by quantitative real-time PCR. Relative expression was determined against GAPDH mRNA levels. Values represent mean ± S.E.M. of four independent experiments. Two-way analysis of variance (ANOVA) and then Tukey's for specific pairwise comparisons were performed for statistical analysis (**c, d**) and independent *t*-test (**e, f**). $*P<0.05$, $**P<0.01$ and $***P<0.001$ compared with the control-untreated cells

induce neuronal cell death in the presynaptic region of the aging cortex [71], in neonatal cardiomyocytes [72], and in dopaminergic neurons within the nigrostriatal circuit [73]. Studies of lung adenocarcinoma report that MFN2 overexpression induces G0/G1 phase arrest and leads to delayed cell proliferation [74–76]. Other research shows that OPA1 maintains inner-mitochondrial membrane morphology and structure with high mRNA expression levels in retina, brain, liver, heart and pancreas [77]. Previous study reported that OPA1 regulated cytochrome *c* release during apoptosis through the mitochondrial rhomboid protease PARL [78]. Furthermore, OPA1-associated Charcot-Marie-Tooth peripheral neuropathy (CMT2A) is thought to be related to mitochondrial plasticity [79]. By time-lapse microscopy of individual neurons, mitochondrial fusion was shown to be impaired in the presence of higher concentrations of dexamethasone. Taken together, these data suggest that an imbalance of mitochondrial dynamics contributed to suppress neuronal proliferation in dexamethasone-treated cells.

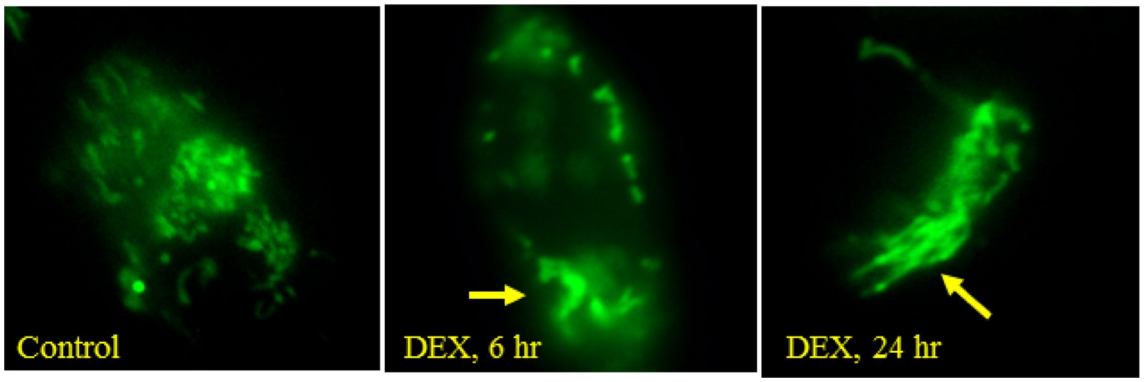

Fig. 11 Mitochondrial morphology effect of dexamethasone-treated neuronal SH-SY5Y cells. SH-SY5Y cells labeled with MitoTracker®Green were imaged with the Cell^R image of confocal microscope

To address concerns with mitophagy, a key process in the mitochondrial quality control system and the clearance of damaged mitochondria have been involved multiple studies of PINK1 and PARKIN [80–82]. PINK1 protein accumulates on mitochondria via its kinase domain, and recruits PARKIN for degradation by mitophagy [83]. PINK1 can acts upstream from Parkin in a mechanism that regulates mitochondrial morphology. It has been shown to prevent neuronal cell death induced by various factors such as oxidative stress [84–86] and excitotoxicity [87]. In response to dexamethasone exposure, there is upregulation of PINK1 and PARKIN mRNA expressions at an earlier stage, thus supporting the view that glucocorticoids change mitophagy genes [88]. Consistent with this, there is upregulation of PARKIN mRNA and protein expression in response to cellular stress [89]. The findings in the present study, suggest that upregulation of PINK1 and PARKIN might represent a cellular adaptation to dexamethasone treatment. Moreover, the expression of PINK1 protein levels does not reflect the mRNA levels, suggesting a complicated mechanism involving in both transcription and translation in response to cellular stress.

Conclusions

Dexamethasone treatment significantly increased mitochondrial ROS formation, and decreased ATP content in SH-SY5Y cells. In particular, dexamethasone modulated mitochondrial fusion that was characterized by tubular shapes. Furthermore, the high concentration of dexamethasone contributed to the suppression of neuronal proliferation. The toxicity of dexamethasone appears to be based not only on its toxic effect on neuronal function, but also on an impairment of the nervous system leading to neuronal death processes.

Acknowledgements This work was supported by a research grant from Mahidol University and the Thailand Research Fund (TRF) under a research Grant for new scholar (MRG5980032), the Higher Education Commission, Mahidol University, under the National Research Universities Initiative. Part of this work was carried out during the tenure of S. Wilasinee as a visiting fellow of the Institute of Translational Research in Biomedicine, Kaohsiung Chang Gung Memorial Hospital, Taiwan, supported by the Committee for Aid and Education in Neurochemistry of the International Society for Neurochemistry and Chang Gung Medical Foundation (OMRPG8C0021) under the sponsorship of Professsors Julie Y.H. Chan and Samuel H.H. Chan.

References

1. Haynes LE, Barber D, Mitchell IJ (2004) Chronic antidepressant medication attenuates dexamethasone-induced neuronal death and sublethal neuronal damage in the hippocampus and striatum. Brain Res 1026:157–167
2. Jacobs CM, Trinh MD, Rootwelt T, Lomo J, Paulsen RE (2006) Dexamethasone induces cell death which may be blocked by NMDA receptor antagonists but is insensitive to Mg^{2+} in cerebellar granule neurons. Brain Res 1070:116–123
3. Tazik S, Johnson S, Lu D, Johnson C, Youdim MB, Stockmeier CA, Ou XM (2009) Comparative neuroprotective effects of rasagiline and aminoindan with selegiline on dexamethasone-induced brain cell apoptosis. Neurotox Res 15:284–290
4. Almeida OF, Conde GL, Crochemore C, Demeneix BA, Fischer D, Hassan AH, Meyer M, Holsboer F, Michaelidis TM (2000) Subtle shifts in the ratio between pro- and antiapoptotic molecules after activation of corticosteroid receptors decide neuronal fate. FASEB J 14:779–790
5. Zuloaga DG, Carbone DL, Quihuis A, Hiroi R, Chong DL, Handa RJ (2012) Perinatal dexamethasone-induced alterations in apoptosis within the hippocampus and paraventricular nucleus of the hypothalamus are influenced by age and sex. J Neurosci Res 90:1403–1412
6. Chen H, Chan DC (2009) Mitochondrial dynamics–fusion, fission, movement, and mitophagy–in neurodegenerative diseases. Hum Mol Genet 18:R169–R176
7. Frezza C, Cipolat S, Martins de Brito O, Micaroni M, Beznoussenko GV, Rudka T, Bartoli D, Polishuck RS, Danial NN, De Strooper B, Scorrano L (2006) OPA1 controls apoptotic cristae remodeling independently from mitochondrial fusion. Cell 126:177–189

8. Qian W, Choi S, Gibson GA, Watkins SC, Bakkenist CJ, Van Houten B (2012) Mitochondrial hyperfusion induced by loss of the fission protein Drp1 causes ATM-dependent G2/M arrest and aneuploidy through DNA replication stress. J Cell Sci 125:5745–5757
9. Shutt T, Geoffrion M, Milne R, McBride HM (2012) The intracellular redox state is a core determinant of mitochondrial fusion. EMBO Rep 13:909–915
10. Theurey P, Rieusset J (2017) Mitochondria-associated membranes response to nutrient availability and role in metabolic diseases. Trend Endocrinol Metab 28:32–45
11. Guo JL, Narasimhan S, Changolkar L, He Z, Stieber A, Zhang B, Gathagan RJ, Iba M, McBride JD, Trojanowski JQ, Lee VM (2016) Unique pathological tau conformers from Alzheimer's brains transmit tau pathology in nontransgenic mice. J Exp Med 213:2635–2654
12. Choong CJ, Mochizuki H (2017) Inappropriate trafficking of damaged mitochondria in Parkinson's disease. Stem Cell Investig 4:17
13. Milakovic T, Quintanilla RA, Johnson GV (2006) Mutant huntingtin expression induces mitochondrial calcium handling defects in clonal striatal cells: functional consequences. J Biol Chem 281:34785–34795
14. Allen J, Romay-Tallon R, Brymer KJ, Caruncho HJ, Kalynchuk LE (2018) Mitochondria and mood: mitochondrial dysfunction as a key player in the manifestation of depression. Front Neurosci 12:386
15. Zager R, Johnson ACM, Becker K (2014) Renal cortical pyruvate depletion during AKI. J Am Soc Nephrol 5:998–1012
16. Suwanjang W, Abramov AY, Charngkaew K, Govitrapong P, Chetsawang B (2016) Melatonin prevents cytosolic calcium overload, mitochondrial damage and cell death due to toxically high doses of dexamethasone-induced oxidative stress in human neuroblastoma SH-SY5Y cells. Neurochem Int 97:34–41
17. Wang Y, Wu M, Gu L, Li X, He J, Zhou L, Tong A, Shi J, Zhu H, Xu J, Guo G (2017) Effective improvement of the neuroprotective activity after spinal cord injury by synergistic effect of glucocorticoid with biodegradable amphipathic nanomicelles. Drug Deliv 24:391–401
18. Kwiecien JM, Jarosz B, Oakden W, Klapec M, Stanisz GJ, Delaney KH, Kotlinska-Hasiec E, Janik R, Rola R, Dabrowski W (2016) An in vivo model of anti-inflammatory activity of subdural dexamethasone following the spinal cord injury. Neurol Neurochir Polska 50:7–15
19. Lee IN, Cheng WC, Chung CY, Lee MH, Lin MH, Kuo CH, Weng HH, Yang JT (2015) Dexamethasone reduces brain cell apoptosis and inhibits inflammatory response in rats with intracerebral hemorrhage. J Neurosci Res 93:178–188
20. Xiao C, Zhou Q, Li X, Li H, Zhong Y, Meng T, Zhu M, Sun H, Liu S, Tang R, Pu J, Xu Y, Xiao P (2017) Losartan and Dexamethasone may inhibit chemotaxis to reduce the infiltration of Th22 cells in IgA nephropathy. Int Immunopharmacol 42:203–208
21. Ismail FS, Moinfar Z, Prochnow N, Dambach H, Hinkerohe D, Haase CG, Forster E, Faustmann PM (2016) Dexamethasone and levetiracetam reduce hetero-cellular gap-junctional coupling between F98 glioma cells and glial cells in vitro. J Neuro-Oncol 131:469–476
22. Abadia B, Calvo P, Ferreras A, Bartol F, Verdes G, Pablo L (2016) Clinical Applications of Dexamethasone for Aged Eyes. Drugs aging 33:639–646
23. Suwanjang W, Abramov AY, Govitrapong P, Chetsawang B (2013) Melatonin attenuates dexamethasone toxicity-induced oxidative stress, calpain and caspase activation in human neuroblastoma SH-SY5Y cells. J Steroid Biochem Molecular Biol 138:116–122
24. Tsujimoto K, Ono T, Sato M, Nishida T, Oguma T, Tadakuma T (2005) Regulation of the expression of caspase-9 by the transcription factor activator protein-4 in glucocorticoid-induced apoptosis. J Biol Chem 280:27638–27644
25. Molitoris JK, McColl KS, Swerdlow S, Matsuyama M, Lam M, Finkel TH, Matsuyama S, Distelhorst CW (2011) Glucocorticoid elevation of dexamethasone-induced gene 2 (Dig2/RTP801/REDD1) protein mediates autophagy in lymphocytes. J Biol Chem 286:30181–30189
26. Spang C, Chen J, Backman LJ (2016) The tenocyte phenotype of human primary tendon cells in vitro is reduced by glucocorticoids. BMC Musculoskelet Disord 17:467
27. Chang LH, Wu SC, Chen CH, Wang GJ, Chang JK, Ho ML (2016) Parathyroid hormone 1–34 reduces dexamethasone-induced terminal differentiation in human articular chondrocytes. Toxicology 368–369:116–128
28. Guo S, Mao L, Ji F, Wang S, Xie Y, Fei H, Wang XD (2016) Activating AMP-activated protein kinase by an alpha1 selective activator compound 13 attenuates dexamethasone-induced osteoblast cell death. Biochem Biophys Res Commun 471:545–552
29. Alqaryyan M, Kilarkaje N, Mouihate A, Al-Bader MD (2016) Dexamethasone-induced intrauterine growth restriction is associated with altered expressions of metastasis tumor antigens and cell cycle control proteins in rat placentas. Reprod Sci 24:1164–1175
30. Lanshakov DA, Sukhareva EV, Kalinina TS, Dygalo NN (2016) Dexamethasone-induced acute excitotoxic cell death in the developing brain. Neurobiol Dis 91:1–9
31. El Zaoui I, Behar-Cohen F, Torriglia A (2015) Glucocorticoids exert direct toxicity on microvasculature: analysis of cell death mechanisms. Toxicol Sci 143:441–453
32. Ichinohashi Y, Sato Y, Saito A, Ito M, Watanabe K, Hayakawa M, Nakanishi K, Wakatsuki A, Oohira A (2013) Dexamethasone administration to the neonatal rat results in neurological dysfunction at the juvenile stage even at low doses. Early Hum Dev 89:283–288
33. Li SX, Fujita Y, Zhang JC, Ren Q, Ishima T, Wu J, Hashimoto K (2014) Role of the NMDA receptor in cognitive deficits, anxiety and depressive-like behavior in juvenile and adult mice after neonatal dexamethasone exposure. Neurobiol Dis 62:124–134
34. Li Z, Jo J, Jia JM, Lo SC, Whitcomb DJ, Jiao S, Cho K, Sheng M (2010) Caspase-3 activation via mitochondria is required for long-term depression and AMPA receptor internalization. Cell 141:859–871
35. Luo M, Lu Z, Sun H, Yuan K, Zhang Q, Meng S, Wang F, Guo H, Ju X, Liu Y, Ye T, Lu Z, Zhai Z (2010) Nuclear entry of active caspase-3 is facilitated by its p3-recognition-based specific cleavage activity. Cell Res 20:211–222
36. Garcia-Faroldi G, Melo FR, Ronnberg E, Grujic M, Pejler G (2013) Active caspase-3 is stored within secretory compartments of viable mast cells. J Immunol 191:1445–1452
37. Suwanjang W, Holmstrom KM, Chetsawang B, Abramov AY (2013) Glucocorticoids reduce intracellular calcium concentration and protects neurons against glutamate toxicity. Cell Calcium 53:256–263
38. Ortega-Martinez S (2015) Dexamethasone acts as a radiosensitizer in three astrocytoma cell lines via oxidative stress. Redox Biol 5:388–397
39. Park J, HO D, Kin H, Lee C, Oark S, Kim Y, Son I, Seol W (2013) Dexamethasone induces the expression of LRRK2 and α-synuclein, two genes that when mutated cause Parkinson's disease in an autosomal dominant manner. BMB Rep 46:454–459
40. Laane E, Panaretakis T, Pokrovskaja K, Buentke E, Corcoran M, Soderhall S, Heyman M, Mazur J, Zhivotovsky B, Porwit A, Grander D (2007) Dexamethasone-induced apoptosis in acute lymphoblastic leukemia involves differential regulation of Bcl-2 family members. Haematologica 92:1460–1469
41. Abrams MT, Robertson NM, Yoon K, Wickstrom E (2004) Inhibition of glucocorticoid-induced apoptosis by targeting the major

splice variants of BIM mRNA with small interfering RNA and short hairpin RNA. J Biol Chem 279:55809–55817
42. Surin AM, Gorbacheva LR, Savinkova IG, Sharipov RR, Khodorov BI, Pinelis VG (2014) Study on ATP concentration changes in cytosol of individual cultured neurons during glutamate-induced deregulation of calcium homeostasis. Biochem Biokhim 79:146–157
43. Lovatt D, Xu Q, Liu W, Takano T, Smith NA, Schnermann J, Tieu K, Nedergaard M (2012) Neuronal adenosine release, and not astrocytic ATP release, mediates feedback inhibition of excitatory activity. Proc Natl Acad Sci USA 109:6265–6270
44. Jiang D, Shi S, Zhang L, Liu L, Ding B, Zhao B, Yagnik G, Zhou F (2013) Inhibition of the Fe(III)-catalyzed dopamine oxidation by ATP and its relevance to oxidative stress in Parkinson's disease. ACS Chem Neurosci 4:1305–1313
45. Teepker M, Anthes N, Fischer S, Krieg JC, Vedder H (2007) Effects of oxidative challenge and calcium on ATP-levels in neuronal cells. Neurotoxicology 28:19–26
46. Rolyan H, Liu S, Hoeijmakers JG, Faber CG, Merkies IS, Lauria G, Black JA, Waxman SG (2016) A painful neuropathy-associated Nav1.7 mutant leads to time-dependent degeneration of small-diameter axons associated with intracellular Ca2 + dysregulation and decrease in ATP levels. Mol Pain. https://doi.org/10.1177/1744806916674472
47. Moreira PI, Carvalho C, Zhu X, Smith MA, Perry G (2010) Mitochondrial dysfunction is a trigger of Alzheimer's disease pathophysiology. Biochim Biophys Acta 1802:2–10
48. Zhang C, Rissman RA, Feng J (2015) Characterization of ATP alternations in an Alzheimer's disease transgenic mouse model. J Alzheimer's Dis 44:375–378
49. Beck SJ, Guo L, Phensy A, Tian J, Wang L, Tandon N, Gauba E, Lu L, Pascual JM, Kroener S, Du H (2016) Deregulation of mitochondrial F1FO-ATP synthase via OSCP in Alzheimer's disease. Nature communications 7:11483
50. Moon HE, Paek SH (2015) Mitochondrial dysfunction in Parkinson's disease. Exp Neurobiol 24:103–116
51. Hu Q, Wang G (2016) Mitochondrial dysfunction in Parkinson's disease. Transl Neurodegener 5:14
52. Murphy MP (2009) How mitochondria produce reactive oxygen species. Biochem J 417:1–13
53. Kandimalla R, Reddy PH (2016) Multiple faces of dynamin-related protein 1 and its role in Alzheimer's disease pathogenesis. Biochim Biophys Acta 1862:814–828
54. Bertholet AM, Delerue T, Millet AM, Moulis MF, David C, Daloyau M, Arnaune-Pelloquin L, Davezac N, Mils V, Miquel MC, Rojo M, Belenguer P (2016) Mitochondrial fusion/fission dynamics in neurodegeneration and neuronal plasticity. Neurobiol Dis 90:3–19
55. Bose A, Beal MF (2016) Mitochondrial dysfunction in Parkinson's disease. J Neurochem 139(Suppl 1):216–231
56. Knott AB, Bossy-Wetzel E (2008) Impairing the mitochondrial fission and fusion balance: a new mechanism of neurodegeneration. Ann N Y Acad Sci 1147:283–292
57. Cho DH, Nakamura T, Lipton SA (2010) Mitochondrial dynamics in cell death and neurodegeneration. Cell Mol Life Sci 67:3435–3447
58. Satapati S, Kucejova B, Duarte JA, Fletcher JA, Reynolds L, Sunny NE, He T, Nair LA, Livingston KA, Fu X, Merritt ME, Sherry AD, Malloy CR, Shelton JM, Lambert J, Parks EJ, Corbin I, Magnuson MA, Browning JD, Burgess SC (2015) Mitochondrial metabolism mediates oxidative stress and inflammation in fatty liver. J Clin Invest 125:4447–4462
59. Vasquez-Trincado C, Garcia-Carvajal I, Pennanen C, Parra V, Hill JA, Rothermel BA, Lavandero S (2016) Mitochondrial dynamics, mitophagy and cardiovascular disease. J Physiol 594:509–525
60. Biala AK, Dhingra R, Kirshenbaum LA (2015) Mitochondrial dynamics: Orchestrating the journey to advanced age. J Mol Cell Cardiol 83:37–43
61. Cho B, Cho HM, Kim HJ, Jeong J, Park SK, Hwang EM, Park JY, Kim WR, Kim H, Sun W (2014) CDK5-dependent inhibitory phosphorylation of Drp1 during neuronal maturation. Exp Mol Med 46:e105
62. Yu T, Jhun B, TYoon Y (2012) High-glucose stimulation increases reactive oxygen species production through the calcium and mitogen-activated protein kinase-mediated activation of mitochondrial fission. Antioxid Redox Signal 14:425–437
63. Kashatus JA, Nascimento A, Myers LJ, Sher A, Byrne FL, Hoehn KL, Counter CM, Kashatus DF (2015) Erk2 phosphorylation of Drp1 promotes mitochondrial fission and MAPK-driven tumor growth. Mol Cell 57:537–551
64. Parameyong A, Govitrapong P, Chetsawang B (2015) Melatonin attenuates the mitochondrial translocation of mitochondrial fission proteins and Bax, cytosolic calcium overload and cell death in methamphetamine-induced toxicity in neuroblastoma SH-SY5Y cells. Mitochondrion 24:1–8
65. Park JH, Ko J, Hwang J, Koh HC (2015) Dynamin-related protein 1 mediates mitochondria-dependent apoptosis in chlorpyrifos-treated SH-SY5Y cells. Neurotoxicology 51:145–157
66. Parone PA, James DI, Da Cruz S, Mattenberger Y, Donze O, Barja F, Martinou JC (2006) Inhibiting the mitochondrial fission machinery does not prevent Bax/Bak-dependent apoptosis. Mol Cell Biol 26:7397–7408
67. Kageyama Y, Zhang Z, Roda R, Fukaya M, Wakabayashi J, Wakabayashi N, Kensler TW, Reddy PH, Iijima M, Sesaki H (2012) Mitochondrial division ensures the survival of postmitotic neurons by suppressing oxidative damage. J Cell Biol 197:535–551
68. Yoon Y, Krueger EW, Oswald BJ, M.A.M (2003) The mitochondrial protein hFis1 regulates mitochondrial fission in mammalian cells through an interaction with the dynamin-like protein DLP1. Mol Cell Biol 23:5409–5420
69. Zorzano A, Hernandez-Alvarez MI, Palacin M, Mingrone G (2010) Alterations in the mitochondrial regulatory pathways constituted by the nuclear co-factors PGC-1alpha or PGC-1beta and mitofusin 2 in skeletal muscle in type 2 diabetes. Biochim Biophys Acta 1797:1028–1033
70. Zorzano A, Liesa M, Palacin M (2009) Mitochondrial dynamics as a bridge between mitochondrial dysfunction and insulin resistance. Arch Physiol Biochem 115:1–12
71. Hara Y, Yuk F, Puri R, Janssen WG, Rapp PR, Morrison JH (2014) Presynaptic mitochondrial morphology in monkey prefrontal cortex correlates with working memory and is improved with estrogen treatment. Proc Natl Acad Sci USA 111:486–491
72. Shen T, Zheng M, Cao C, Chen C, Tang J, Zhang W, Cheng H, Chen KH, Xiao RP (2007) Mitofusin-2 is a major determinant of oxidative stress-mediated heart muscle cell apoptosis. J Biol Chem 282:23354–23361
73. Pham AH, Meng S, Chu QN, Chan DC (2012) Loss of Mfn2 results in progressive, retrograde degeneration of dopaminergic neurons in the nigrostriatal circuit. Hum Mol Genet 21:4817–4826
74. Lou Y, Li R, Liu J, Zhang Y, Zhang X, Jin B, Liu Y, Wang Z, Zhong H, Wen S, Han B (2015) Mitofusin-2 over-expresses and leads to dysregulation of cell cycle and cell invasion in lung adenocarcinoma. Med Oncol 32:132
75. Rehman J, Zhang HJ, Toth PT, Zhang Y, Marsboom G, Hong Z, Salgia R, Husain AN, Wietholt C, Archer SL (2012) Inhibition of mitochondrial fission prevents cell cycle progression in lung cancer. FASEB J 26:2175–2186
76. Chen K, Guo X, Ma D, Guo Y, Li Q, Yang D, Li P, Qiu X, Wen S, Xiao R, Tang J (2004) Dysregulation of HSG triggers vascular proliferative disorders. Nat Cell Biol 6:872–883

77. Olichon A, Guillou E, Delettre C, Landes T, Arnaune-Pelloquin L, Emorine LJ, Mils V, Daloyau M, Hamel C, Amati-Bonneau P, Bonneau D, Reynier P, Lenaers G, Belenguer P (2006) Mitochondrial dynamics and disease, OPA1. Biochim Biophys Acta 1763:500–509
78. Cipolat S, Rudka T, Hartmann D, Costa V, Serneels L, Craessaerts K, Metzger K, Frezza C, Annaert W, D'Adamio L, Derks C, Dejaegere T, Pellegrini L, D'Hooge R, Scorrano L, De Strooper B (2006) Mitochondrial rhomboid PARL regulates cytochrome c release during apoptosis via OPA1-dependent cristae remodeling. Cell 126:163–175
79. Amati-Bonneau P, Milea D, Bonneau D, Chevrollier A, Ferre M, Guillet V, Gueguen N, Loiseau D, de Crescenzo MA, Verny C, Procaccio V, Lenaers G, Reynier P (2009) OPA1-associated disorders: phenotypes and pathophysiology. Int J Biochem Cell Biol 41:1855–1865
80. Ashrafi G, Schwarz TL (2013) The pathways of mitophagy for quality control and clearance of mitochondria. Cell Death Differ 20:31–42
81. Hattori N, Saiki S, Imai Y (2014) Regulation by mitophagy. Int J Biochem Cell Biol 53:147–150
82. Scarffe LA, Stevens DA, Dawson VL, Dawson TM (2014) Parkin and PINK1: much more than mitophagy. Trends Neurosci 37:315–324
83. Whitworth AJ, Pallanck LJ (2009) The PINK1/Parkin pathway: a mitochondrial quality control system? J Bioenerg Biomembr 41:499–503
84. Kitagishi Y, Nakano N, Ogino M, Ichimura M, Minami A, Matsuda S (2017) PINK1 signaling in mitochondrial homeostasis and in aging (Review). Int J Mol Med 39:3–8
85. Li L, Hu GK (2015) Pink1 protects cortical neurons from thapsigargin-induced oxidative stress and neuronal apoptosis. Biosci Rep 35:e00174
86. Cang X, Wang X, Liu P, Wu X, Yan J, Chen J, Wu G, Jin Y, Xu F, Su J, Wan C, Wang X (2016) PINK1 alleviates palmitate induced insulin resistance in HepG2 cells by suppressing ROS mediated MAPK pathways. Biochem Biophys Res Commun 478:431–438
87. Rosen KM, Veereshwarayya V, Moussa CE, Fu Q, Goldberg MS, Schlossmacher MG, Shen J, Querfurth HW (2006) Parkin protects against mitochondrial toxins and beta-amyloid accumulation in skeletal muscle cells. J Biol Chem 281:12809–12816
88. Troncoso R, Paredes F, Parra V, Gatica D, Vasquez-Trincado C, Quiroga C, Bravo-Sagua R, Lopez-Crisosto C, Rodriguez AE, Oyarzun AP, Kroemer G, Lavandero S (2014) Dexamethasone-induced autophagy mediates muscle atrophy through mitochondrial clearance. Cell cycle 13:2281–2295
89. Wang HQ, Imai Y, Kataoka A, Takahashi R (2007) Cell type-specific upregulation of Parkin in response to ER stress. Antioxid Redox Signal 9:533–542